Еуразиялық агротехникалық журнал = Евразийский агротехнический журнал. – Астана: С. Сейфуллин атындағы Қазақ агротехникалық зерттеу университеті, 2026. -№ 1 (129). - P.-123-143. - ISSN 3135-243X, 3135-2448

doi.org/10.51452/eaj.2026.1(129).2124
UDC 631.432.2; 551.4; 528.856 **Research article**

Relief variation influence on soil moisture in agrofields in Northern Kazakhstan

Berik Rakhimzhanov[1], Alexander Sidorik[2]

[1] Darkan-Dala Agrochemical Laboratory, Astana, Kazakhstan
[2] Olzha Agro, Qostanai, Kazakhstan

Corresponding author: Berik Rakhimzhanov: rahimzhanovberik@gmail.com
Co-authors: (1: AS) s4zqgm@gmail.com
Received: 26 January 2026 **Accepted:** 17 March 2026 **Published:** 30 March 2026

Abstract

Background and Aim. As a result of the Soviet land resource planning system, large agrofields in Northern Kazakhstan have historically been delineated by administrative boundaries rather than relief characteristics, which can impact soil moisture heterogeneity under semi-arid conditions. This study aims to quantify how micro-relief variability controls soil moisture distribution within a representative chernozem field using UAV-derived terrain data and in-situ soil moisture telemetry.

Materials and Methods.The study was conducted in test Field No. 64 (440 ha), Kostanay region, Kazakhstan. The high-resolution Digital Terrain Models were generated from UAV photogrammetry (Mavic 2 Pro; August 2024) and used to characterize elevation gradients. The six Sentek Drill & Drop probes (0-60 cm, 10 cm intervals) were installed within the elevation range and recorded volumetric water content at 30-minute intervals from May-September 2025, the telemetry from sensors was quality-controlled and aggregated to monthly means. Elevation effects were assessed to determine relationships for each month and depth horizon using Pearson and Spearman correlations and ordinary least-squares regression (VWC = a + b•Elevation).

Results. Despite a small elevation span (~3 m at probe locations), monthly mean soil moisture exhibited consistent moderate associations with elevation, particularly in the early season and deeper horizons. Statistically significant Pearson relationships ($p < 0.05$) were observed for May at 10-20 cm ($r = -0.95$; $b = -3.03$% VWC per m; $R^2 = 0.90$), 20-30 cm ($r = -0.91$; $b = -1.87$% per m; $R^2 = 0.83$), and 50-60 cm ($r = -0.86$; $b = -2.08$% per m; $R^2 = 0.73$). In June, significant effects persisted at 40-50 cm ($r = -0.86$; $b = -1.47$% per m; $R^2 = 0.74$) and 50-60 cm ($r = -0.93$; $b = -2.67$% per m; $R^2 = 0.86$), and in July at 50-60 cm ($r = -0.85$; $b = -1.82$% per m; $R^2 = 0.72$), indicating systematically wetter conditions at lower microtopographic positions.

Conclusion. Integrating UAV-derived terrain metrics with depth-resolved soil moisture telemetry enables detection of meaningful micro-topographic controls on root-zone water availability within large steppe agrofields. The identified elevation–moisture gradients can support within-field zoning, targeted water-conservation practices, and more robust interpretation of remote-sensing soil moisture products in Northern Kazakhstan.

Keywords: Soil; moisture; relief height segmentation; soil moisture telemetry; UAV scanning the agrofields; North Kazakhstan.

Introduction

Productive moisture, defined as the portion of water in the soil accessible for plant uptake, is critical for maintaining plant growth and synthesizing organic matter. In Northern Kazakhstan, the thermal regimedoes not typically limit the growth and development of grain crops. Instead, the availability of atmospheric precipitation, which influences the reserves of soil moisture during the growing season, is the primary factor determining productivity [1]. Research has shown that in the dry steppe zone, each millimeter of soil moisture contributes to the formation of up to 14 kg of grain, while summer precipitation contributes 12.2 kg per mm [2, 3]. These results highlight the critical importance of effective water management in agricultural systems.

Against this backdrop, investigating the influence of topographical variation on soil moisture distribution becomes a pressing scientific and practical concern. Remote sensing technologies and UAV-derived digital terrain models (DTM) now provide powerful tools for studying these dynamics [4, 5]. Rapid and accurate estimation of crop root zone soil moisture (RZSM) is critical for precision agricultural water management, especially in arid and semi-arid regions [6]. Understanding the correlations between topography and soil moisture has the potential to guide sustainable agricultural practices, optimize water resource management, and enhance crop resilience in arid environments.

In Kazakhstan, the total available land area is estimated approximately 32 mln ha. More than 55% of that area is located in the dry steppe zone. Kazakhstan's soil is represented by Chernozem with a humus content of 3 to 6% [7]. Chernozem is located in the Northern, Eastern, and Central parts of the country. The South Chernozem in North Kazakhstan occupies 25.3 mln ha and is the most productive soil in the country. An area of approximately 11 mln ha of Chernozem soil was planted rather with spring wheat (*Triticum aestivum* L).

Paradoxically, while the Soviet Union was widely recognized for its advancements in soil science, including pioneering research on soil fertility, water retention, and land management, the practical application of these findings often fell short in large-scale agricultural projects. The theoretical and experimental groundwork laid by Soviet soil scientists provided detailed insights into the relationship between topographical relief and soil moisture dynamics. However, these contributions were frequently overlooked in practice, particularly in state-driven campaigns such as the Virgin Lands initiative.

Soviet researchers extensively studied the impact of relief variations on soil moisture distribution, leveraging field experiments, mathematical modeling, and laboratory simulation. For example, the work of *V. Dokuchaev*, often regarded as the founder of soil science, established the foundational understanding of how topographical and climatic conditions influence soil formation processes [14]. His principles were expanded upon in later decades by scholars like *K.K. Gedroits*, who investigated soil moisture dynamics about capillary action and water retention capacity across different soil types [9].

The research of *G.V. Dobrovolsky* focused on soil hydrology, particularly the role of microrelief in regulating moisture distribution within arid and semi-arid landscapes [5]. His studies highlighted the critical importance of slope gradients in influencing infiltration rates and water storage capacity.

One notable contribution comes from *A.A. Rode*, whose work emphasized the interaction between slope processes and soil erosion, further linking relief variations to water availability. *Rode's* studies in Central Asia provided practical recommendations for land management in semi-arid regions, advocating for contour plowing and the creation of terraces to maximize moisture retention [17].

The legacy of Soviet soil science, however, remains invaluable for modern researchers. Revisiting the extensive work of scholars like *Dokuchaev, Gedroits, Dobrovolsky* and *Rode* offers a wealth of insights into sustainable agricultural practices and resources management. Incorporating these principles into contemporary land-use strategies could address current challenges, such as water scarcity and land degradation, particularly in arid regions like Kazakhstan.

In the Western scientific community numerous studies have explored the intricate relationships between soil moisture dynamics and topographical variations [11]. In arid and semi-arid regions like Northern Kazakhstan, these interactions play a pivotal role in agricultural productivity [12, 13]. Early foundational work by [14] revisited *Richard's* Equation (1931) to model unsaturated hydraulic flow, laying the groundwork for understanding water movements in soils. *Philip* further advanced infiltration theories, emphasizing the importance of gradient-driven hydraulic conductivity [16]. Analysis of capillary tension in unsaturated flow by *W.R Gardner*, was an attempt at a dynamic modelling approach to the issues of soil water content [8].

The Brooks and Corey model remains one of the most influential approaches for describing the relationship between soil moisture and unsaturated hydraulic conductivity [16]. Their methodology, which integrates soil porosity and retention curves, has been extensively validated across diverse soil types. Similarly, *Gardner's* analytical formulations for capillary tension in unsaturated soils remain relevant for predicting soil water retention under varying topographic conditions [17].

Topographical effects were formalized in [18]. TOP model, which links spatial soil moisture variability to elevation gradients. While this model has been widely adopted, its assumption of uniform lateral flow in unsaturated zones has faced critique. *Zaslavsky* and *Sinai* introduced anisotropy considerations, providing insights into lateral moisture redistribution influenced by soil heterogeneity [22]. Their work underscored the need to account for microrelief a critical factor in regions with undulating terrains, like the Kostanay airfields.

Remote sensing technologies have revolutionized soil moisture assessments, offering precise spatial data. *Gelhar* and *Mantoglou* advocated for stochastic modeling to address soil heterogeneity, emphasizing variability in hydraulic conductivity [10]. More recent studies leverage UAV-derived digital terrain models (DTMs) and spectral indices such as NDWI (Normalized Difference Water Index) to quantify soil moisture patterns across topographical gradients. These advancements enable the integration of temporal datasets, aiding in the analysis of seasonal moisture trends.

With the development of UAV technologies, a new approach to collecting the terrain characteristics of the field has become available. As a result, the drones can be instrumental at the start of the crop cycle. They produce precise map data for early soil analysis, which is useful in planning seed planting [21]. Before the planting season, it is necessary to arrange for land monitoring, including the geography of the field [22]. Current limitations in technologies need to be improved, such as imperfect hovering capabilities, constrained flight time and payload [23].

Combining theoretical models with empirical observations, contemporary research highlights the interplay of topography, vegetation cover, and climate variables in modulating soil moisture. The integration of UAV technologies with remote sensing and hydrological models offers unparalleled precision, making it an indispensable tool for modern agroecological research.

Study area description

The research was carried out in study arealocated in the Kostanay region, in the northern part of the Republic of Kazakhstan . Kostanay region located in continental climate conditions in North part of the steppe zone which spans over the vast area of Kazakhstan (Figure 1). Annual precipitation is 300-400 mm and a vegetation period from April to October. The growing season is 150-175 days in the north and 180 days in the south part of region, with the solar activity period of 250 days per year [7]. Traditionally, the main crops are wheat, barley, sunflower.

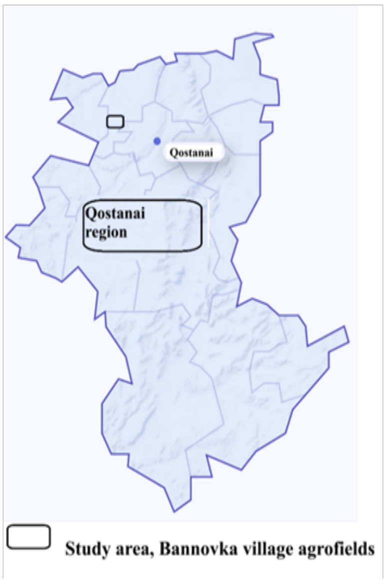

Figure 1 – Study area, Kostanay region of Kazakhstan

According to the Food and Agriculture Organization (FAO) global soil classification framework, the test field is situated within the mapping unit Ch 15-3a [25]. This designation corresponds to a specific soil mapping code used in the FAO's soil legend to denote a distinct combination of soil type, texture, and associated physiographic conditions.

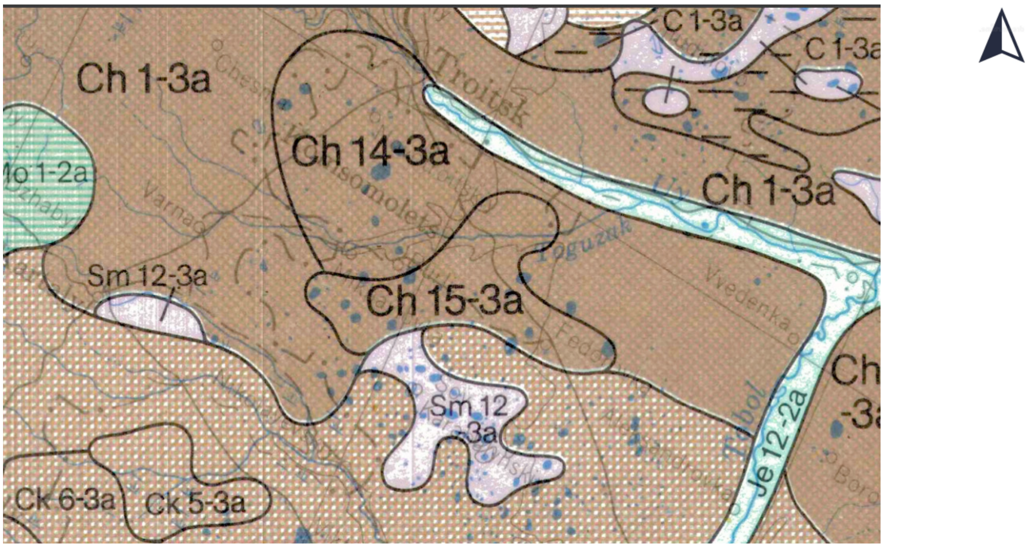

Figure 2 – FAO classification soil type of study area Ch 15-3a

C-Chermozems, Ch-Chaplic Chernozems, 15- North & Central Asia, 3 = fine textured topsoil, a = level to gently undulating slopes (0-8%). Scale: 1: 50 000., maps source: https://www.fao.org/soils-portal/data-hub/soil-maps-and-databases/regional-and-national-soil-maps-and-databases/en/

The soil unit Ch-15-3a corresponds to Haplic Chernozems with a fine-textured (clayey) profile located on level to gently undulating terrain (0-8% slope) (Figure 2). These soils are characterized by a deep, dark mollic horizon rich in organic matter, high base saturation (>50%), strong aggregate structure, and excellent natural fertility. Their fine texture enhances water and nutrient retention, making them highly suitable for intensive agriculture, particularly in temperate steppe regions. Haplic Chernozems, exhibit a well-defined horizon sequence typical of steppe soils formed under grassland vegetation. The uppermost layer is a thick, dark mollic A horizon, rich in organic matter and calcium, with a granular structure, high base saturation (>50%), and neutral to slightly alkaline pH indicating excellent natural fertility. This is followed by a B horizon, where increased clay content and moderate structural development occur due to pedogenic processes such as clay translocation. The deeper Ck horizon contains accumulations of secondary carbonates ($CaCO_3$), often appearing as nodules or filaments. The soil is fine-textured (clayey), has strong aggregation, and forms on level to gently undulating terrain. Its structure promotes good moisture retention and aeration, while the presence of calcium enhances flocculation and root penetration. These characteristics productive and suitable for mechanized dryland farming, especially in temperate continental climates.

Materials and Methods

Field No. 64 located in the Kostanay region of Northern Kazakhstan, spans an area of 440 hectares. The field was surveyed using drone Mavic 2 Pro at the end of August 2024 according to standard procedures for high-resolution topographic and spatial data collection.

During the drone survey, ground control points (GCPs) strategically were placed across the field to ensure accurate georeferencing. The images captured by the the UAV were processed to generate orthophotos and a Digital Elevation Model (DEM). The DEM was subsequently converted into elevation contours, enabling a comprehensive analysis of the field's relief (Figure 3).

Relief Analysis of the Field No.64

The elevation data derived from the DEM were analyzed to quantify the field's topographical variation. The statistical summary of the elevation data is as follows:

- Minimum elevation: 127.96 m;
- Maximum elevation: 135.55 m;
- Elevation range: 7.59 m;

- Average elevation: 131.82 m;
- Standard deviation: 1.13 m.

To further investigate the distribution of the field area by elevation, the data were categorized into 1-meter elevation ranges (Table 1).

Table 1 – Illustrates the distribution of the field area across these elevation ranges

Altitude above the Sea level (m)	Area (ha)	Percentage (%)
< 129	2.3	0.7
129-130	20.1	5.8
130-131	61.8	17.9
131-132	106.3	30.8
132-133	95.4	27.6
>134	59.2	17.2

The largest area, 106.3 hectares (30.8% of the total field area), lies within the 131-132 m elevation range. Other significant ranges include 132-133 m (27.6%) and 130-131 m (17.9%). The lowest elevation range (<129 m) and the highest range (>134 m) cover smaller proportions of the field, accounting for 0.7% and 17.2%, respectively.

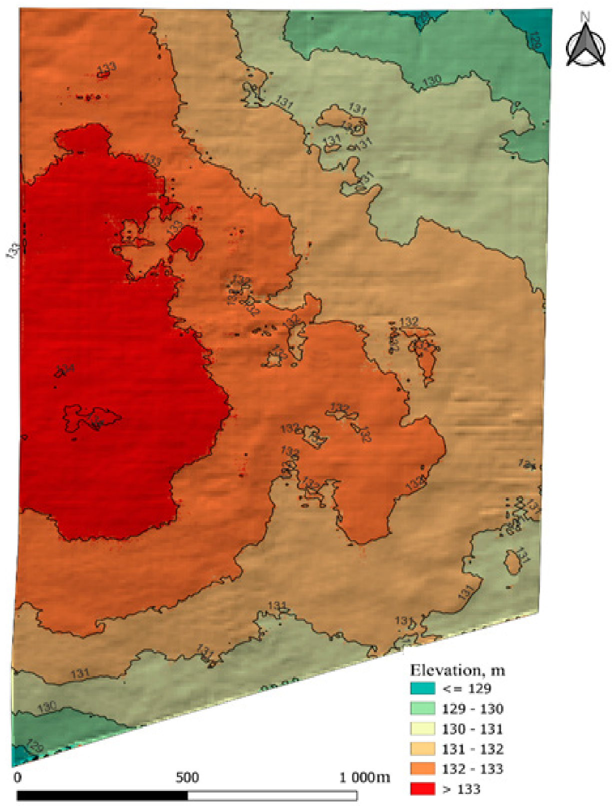

Figure 3 – Field No. 64, Kostanay region, North-West Kazakhstan, Fyodorovka district.
The height of the relief spans from 129 to 133 meter above Sea level in Baltic system of heights

To examine the relationship between topography and other field characteristics, the elevation profile of Field 64 was analyzed in detail. Elevation data were obtained from a high-resolution Digital Elevation Model (DEM) taken by UAV scanning and classified into discrete 1-meter elevation intervals. This classification allowed for a systematic assessment of how the field's surface area is distributed across different altitude bands. The results of this categorization are presented in Figure 4, which provides a quantitative summary of the Field 64 area corresponding to each 1-meter elevation range.

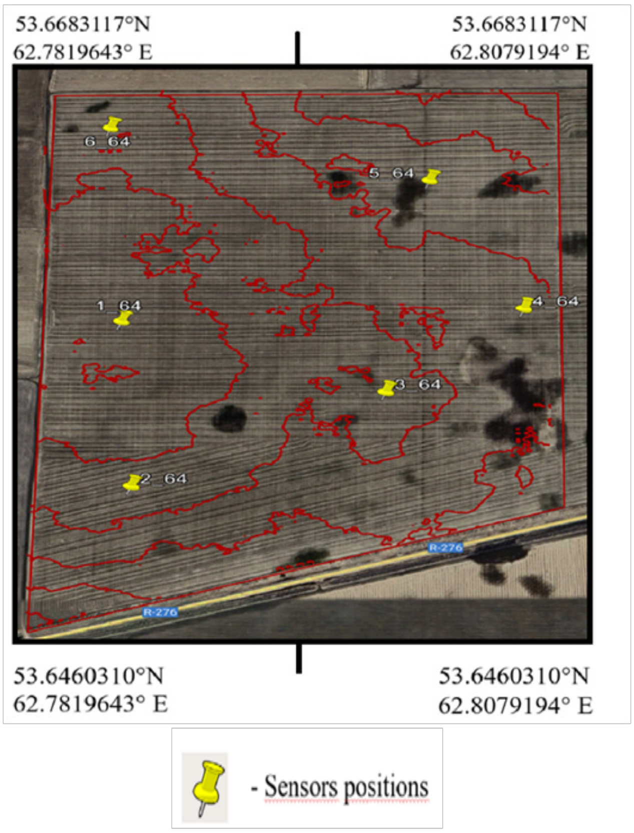

Figure 4 – Position of soil sensor probes and relief heights isolines of the test field

The marginal vertical variability implied by the hypsometry, any representative planar gradient across the field is on the order of 1-5% which is fully corresponds with the FAO classification of undulating slopes 0-8%.

For the purposes of this study, the influence of relief slope characteristics to the soil moisture distribution over the study are the Sentek Drill & Drop-probe soil moisture probes are intentionally positioned across the full range of relief elevations, ensuring spatially representative in-situ measurements.

A total of six soil probe stations were installed in Field 64 on 16 April 2025. The equipment consists of Sentek Drill & Drop-probe soil moisture probes, each installed to a total depth of 60 cm and configured to record measurements at 10 cm intervals.

The soil moisture probes were inserted vertically into the soil profile, enabling simultaneous measurement of volumetric water content and soil temperature at depths of 10, 20, 30, 40, 50, and 60 cm. This installation approach ensures the capture of depth-resolved moisture dynamics within the root zone and subsoil layers, facilitating high-resolution temporal monitoring of soil water status across different micro-topographic positions in the field. In this research we implement of field sectoral study within the 50 m range from the positions of probes as the reliability area (Figure 5). Further Satellite data processing and statistical aggregation of the data sets were located within the 50-meter range study sectors over the field area.

Figure 5 – Sentek Drill & Drop probe for 60 cm depth probe view and installation

Probes were installed in pre-augured holes and good soil-probe contact was ensured using a slurry of sieved native soil and water. Probes were connected to HOBO data loggers configured to record readings every 30 min. Soil temperature data were corrected for thermal lag using adjacent surface measurements and calibrated against air temperature from the meteorological station (Figure 6).

a-Probe # 64-1

b-Probe # 64-2

c-Probe # 64-3

d-Probe # 64-4

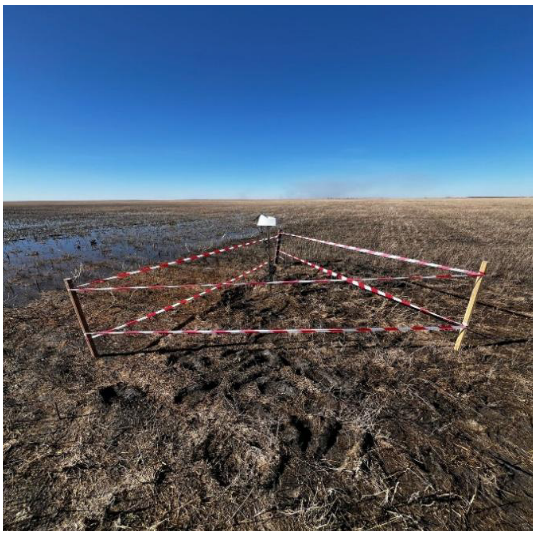

e-Probe # 64-5

f-Probe # 64-6

Figure 6 – Sentek Ground soil probes installation field view
a, b, c, d, e, f - pictures are the positions of the probes in different angle of view

In this study, all in situ soil probes were bench calibrated under laboratory conditions prior to field deployment. Following installation, the probes require an equilibration period of approximately 2-3 weeks for readings to stabilize and for internal self calibration routines to complete. Consequently, by the time of the first field campaign and the coincident satellite acquisitions, the probe records can be treated as stable and reliable for analysis, for the protecting the equipment from external factors, locations were marked by wood sticks and tape (Figure 6).

Telemetry is provided via the GSM cellular network, and measurements are acquired at a 30 min sampling interval. The user facing software allows configurable temporal aggregation, enabling data retrieval as hourly records or as daily averages, and supports export in multiple standard data formats to facilitate downstream processing.

Statistical analysis of in-situ soil-moisture telemetry

Half-hourly volumetric water content (VWC, %) records from the six Sentek Drill & Drop-probes were quality-controlled prior to analysis. Data were screened for missing timestamps and physically implausible values, and short isolated spikes were treated as artefacts and removed using a median-based filter. Because probe readings may drift during the post-installation equilibration period, the first weeks after deployment were not used for inference; subsequent analyses were restricted to May-September 2025 (Appendixes A-F). For each sensor and depth horizon (0-10, 10-20, 20-30, 30-40, 40-50, and 50-60 cm), daily means were calculated and then aggregated to monthly means to provide a robust summary that is less sensitive to high-frequency noise.

To evaluate whether topographic position is associated with soil moisture, the elevation at each probe location was treated as a fixed covariate (user-validated reference heights). For each month and depth horizon, dependence of monthly mean VWC on elevation was quantified using Pearson correlation (linear association), Spearman rank correlation (monotonic association, robust to non-normality and outliers), and ordinary least-squares regression of the form VWC = a + b•Elevation, where the slope b represents the expected change in monthly mean VWC per 1 m elevation difference. Given the small spatial sample size (n = 6 sensors) and the narrow elevation range (~3 m), results are interpreted primarily in terms of effect direction and magnitude, with p-values reported as descriptive evidence rather than definitive hypothesis tests. All statistics were computed independently for each month–horizon combination.

Results and Discussion

Monthly mean volumetric water content (VWC, %) was computed for six soil-moisture sensors across six depth horizons (0-10, 10-20, 20-30, 30-40, 40-50, and 50-60 cm) for May-September 2025. Elevation at each sensor installation point was taken from user-validated reference heights (Table 2-6).

№ 1 (129)/2026 ISSN 3135-243X, 3135-2448

For each month and depth horizon, the dependence of VWC on elevation was quantified using Pearson correlation, Spearman rank correlation, and a simple linear regression model (VWC = a + b•Elevation). Because the analysis is based on n = 6 sensors, the statistical power is limited, statistical power is limited; therefore, the interpretation emphasizes effect direction, magnitude, and cross-month consistency.

Table 2 – Monthly mean VWC (%) by sensor and depth horizon, May 2025

Sensor	Elev. (m)	0-10 cm	10-20 cm	20-30 cm	30-40 cm	40-50 cm	50-60 cm
1_64	133	31.82	42.29	47.10	48.80	49.15	47.99
2_64	132	36.56	46.47	48.55	49.59	49.90	49.77
3_64	132	27.12	44.36	48.30	48.65	49.42	48.79
4_64	131	37.37	48.00	48.76	48.37	49.75	49.14
5_64	130	36.71	51.17	53.20	55.27	50.75	54.81
6_64	132	23.59	43.29	48.37	48.04	46.07	48.53

Table 3 – Monthly mean VWC (%) by sensor and depth horizon, June 2025

Sensor	Elev. (m)	0-10 cm	10-20 cm	20-30 cm	30-40 cm	40-50 cm	50-60 cm
1_64	133	9.02	26.43	38.40	45.15	47.62	46.76
2_64	132	11.16	19.68	30.92	43.46	47.57	48.29
3_64	132	6.88	23.00	32.54	41.84	47.38	47.75
4_64	131	13.76	35.60	47.29	47.93	49.77	49.59
5_64	130	8.29	25.40	43.49	54.68	51.18	55.16
6_64	132	19.73	40.91	47.67	48.01	46.52	49.16

Table 4 – Monthly mean VWC (%) by sensor and depth horizon, July 2025

Sensor	Elev. (m)	0-10 cm	10-20 cm	20-30 cm	30-40 cm	40-50 cm	50-60 cm
1_64	133	8.40	20.40	32.49	40.53	46.59	46.00
2_64	132	10.75	16.34	26.74	40.39	47.07	47.94
3_64	132	6.72	19.49	23.02	32.21	42.78	45.65
4_64	131	12.03	29.06	43.69	46.97	49.07	49.03
5_64	130	7.16	12.32	17.29	26.51	35.63	51.57
6_64	132	18.42	39.34	46.60	47.57	46.38	49.20

Table 5 – Monthly mean VWC (%) by sensor and depth horizon, August 2025

Sensor	Elev. (m)	0-10 cm	10-20 cm	20-30 cm	30-40 cm	40-50 cm	50-60 cm
1_64	133	9.92	17.43	29.63	38.01	46.10	45.55
2_64	132	9.85	12.92	20.64	35.41	46.64	47.82
3_64	132	8.06	19.83	21.50	29.92	40.46	43.32
4_64	131	13.68	24.15	37.71	45.31	48.26	48.36
5_64	130	9.98	11.34	12.40	11.47	17.73	42.29
6_64	132	16.90	35.05	42.87	44.66	44.23	48.25

№ 1 (129)/2026 ISSN 3135-243X,3135-2448

Table 6 – Monthly mean VWC (%) by sensor and depth horizon, September 2025

Sensor	Elev. (m)	0-10 cm	10-20 cm	20-30 cm	30-40 cm	40-50 cm	50-60 cm
1_64	133	14.64	19.90	28.12	35.90	44.93	44.74
2_64	132	15.18	15.51	17.63	31.58	45.63	47.41
3_64	132	12.69	26.44	23.79	30.49	39.60	42.09
4_64	131	16.92	26.78	35.47	42.85	47.36	47.73
5_64	130	13.40	14.54	11.08	10.27	16.28	40.54
6_64	132	17.01	34.68	41.03	42.27	43.14	47.43

Elevation dependence of monthly mean soil moisture.

The elevation–VWC relationship was seasonally and vertically heterogeneous. In May, locations at higher elevations were generally drier, with strong negative associations for 10-20 cm, 20-30 cm, and 50-60 cm. In June and July, the negative relationship with elevation persisted primarily in deeper horizons (40-60 cm). By August and September, shallow horizons (0-20 cm) showed weak and inconsistent associations, whereas intermediate depths (30-50 cm) exhibited a tendency toward higher VWC at higher elevations; however, these late-season positive tendencies were not statistically significant at n = 6and should be considered indicative rather than conclusive.

Month-horizon combinations with Pearson $p < 0.05$ were:

- May 2025, 10-20 cm: r = -0.95, p = 0.004; b = -3.03 % per m, R2 = 0.90.
- May 2025, 20-30 cm: r = -0.91, p = 0.011; b = -1.87 % per m, R2 = 0.83.
- May 2025, 50-60 cm: r = -0.86, p = 0.029; b = -2.08 % per m, R2 = 0.73.
- June 2025, 50-60 cm: r = -0.93, p = 0.008; b = -2.67 % per m, R2 = 0.86.
- June 2025, 40-50 cm: r = -0.86, p = 0.027; b = -1.47 % per m, R2 = 0.74.
- July 2025, 50-60 cm: r = -0.85, p = 0.032; b = -1.82 % per m, R2 = 0.72.

The regression slope b represents the expected change in monthly mean VWC per 1 m increase in elevation. Given the modest elevation range across sensors (130-133 m) and the small spatial sample size, these results may reflect not only topographic effects but also co-varying site factors(e.g., soil texture, microrelief-driven redistribution, and management). Accordingly, elevation should be interpreted as a proxy variable of local setting rather than a standalone causal driver.

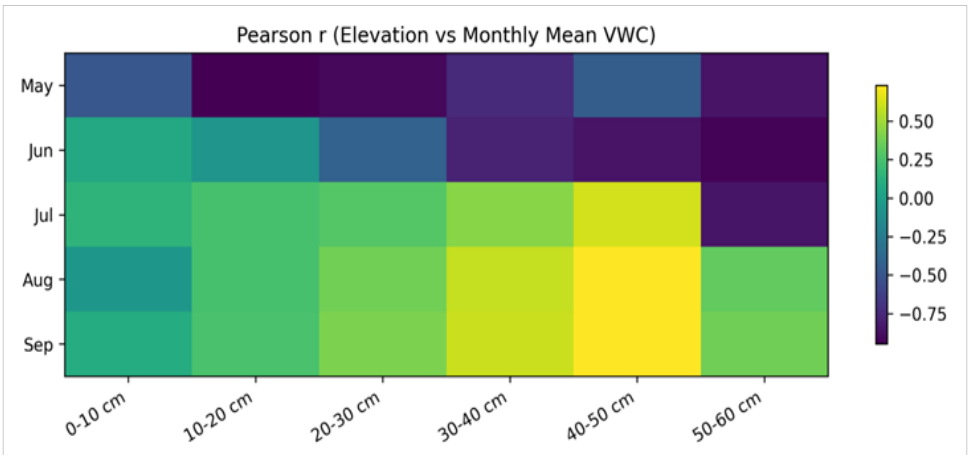

Figure 7 – synthesizes the Pearson correlation coefficients between elevation and monthly mean VWC across depth horizons for May-September 2025

The correlation structure is both seasonally and vertically heterogeneous. In May, higher-elevation locations tended to be drier, with the strongest negative association at 10-20 cm (r = −0.95), followed by 20-30 cm (r = −0.91) and 50-60 cm (r = −0.86). During June-July, negative elevation signals persisted mainly in the deeper horizons (40-60 cm), whereas shallow horizons (0-20 cm) were weak and inconsistent, reflecting stronger control by short-term atmospheric forcing and surface evaporation.

By August-September, correlations at intermediate depths (30-50 cm) shifted toward weak-to-moderate positive values, suggesting that moisture storage in the root-zone/subsoil can differ from near-surface behavior late in the season, however, these late-season tendencies are not robust given the small sample size (n = 6) and should be interpreted as indicative patterns rather than conclusive evidence of a reversal in topographic control.

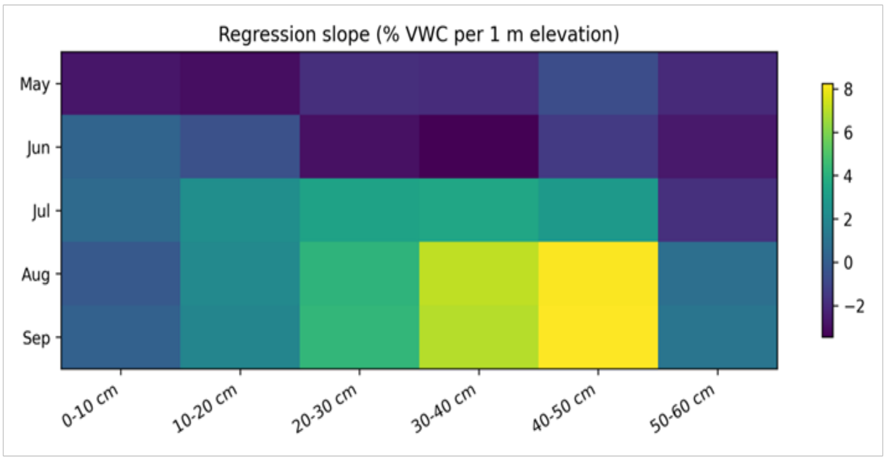

Figure 8 – Presents the linear regression slopes (b) linking elevation to monthly mean VWC for each depth horizon and month

Negative slopes dominate the early part of the growing season, indicating decreasing VWC with increasing elevation, with the largest effect observed in May at 10-20 cm (b = −3.03 % VWC per m; R2 = 0.90). In June, the strongest negative responses occur in the deeper horizons (e.g., 50-60 cm: b = −2.67 % per m;R2 = 0.86), consistent with a persistent elevation gradient in subsoil water storage during the transition to summer drying. In contrast, late-season slopes at intermediate depths (30-50 cm) become small and occasionally positive, implying only modest increases in VWC at higher elevations. Given the limited elevation range across the sensor network (130-133 m), even the largest estimated slopes translate to differences on the order of 6-9 percentage points across the field-scale relief, whereas most month–horizon combinations imply substantially smaller contrasts. Overall, the regression results reinforce that elevation effects are depth-specific and time-dependent, and that relief height alone is unlikely to serve as a standalone predictor providesof moisture status without accounting for co-varying site properties.

Conclusion

This study combined a UAV-derived digital elevation model (DEM) with continuous in-situ measurements from Sentek Drill & Drop probes to examine how modest relief variations in a large dryland field (Field 64) relate to soil moisture dynamics during the 2025 growing season. The hypsometric analysis confirms that the field is quasi-flat, with most of the area concentrated between 130 and 133 m above sea level, yet this seemingly small vertical range is sufficient to create discernible differences in the moisture regime when evaluated at appropriate depths and times.

Monthly depth profiles derived from probe telemetry show a clear vertical stratification of water content: near-surface layers (0-20 cm) exhibit the largest seasonal amplitude and rapid depletion during summer, whereas deeper horizons (40-60 cm) maintain higher and more stable VWC, consistent with their larger storage capacity and weaker coupling to short-term atmospheric demand. This depth-resolved behavior highlights the value of multi-horizon telemetry for interpreting root-zone conditions and for separating transient surface drying from longer-term subsoil water availability.

The elevation-moisture relationship is not monotonic through the season. Early in the season (May), higher-elevation positions were generally drier at several horizons, with statistically strong negative associations at 10-20 cm and 20-30 cm. During June-July, the negative elevation signal was most evident in the deeper layers (40-60 cm), indicating that topographic position may influence subsoil storage as the profile transitions into summer drying. By August-September, intermediate depths (30-50 cm) displayed weak-to-moderate positive tendencies, while the shallow horizons remained inconsistent, suggesting that late-season moisture patterns may be governed by a combination of redistribution processes, soil heterogeneity, and management effects rather than elevation alone. Because the analysis is based on only six point locations and a narrow elevation span, elevation should be viewed as a proxy descriptor of local setting; co-varying factors such as texture, compaction, microrelief-driven runoff/run-on, and residue cover may contribute materially to the observed contrasts.

From an applied perspective, the results support using DEM products as part of a multi-layer diagnostic framework for precision agronomy, particularly when combined with in-situ sensing and remotely sensed moisture indicators (e.g., NDWI). Relief-derived zones can help stratify sampling and guide variable-rate decisions, but the present findings caution against treating elevation as a universal predictor across depths and months. Future work should extend the analysis to multiple years, increase the number of sensor locations, and incorporate additional terrain derivatives (slope, curvature, topographic wetness index) and soil covariates to better isolate causal drivers and improve predictive skill for field-scale moisture mapping in the dry steppe of Northern Kazakhstan.

Authors' Contributions

BR, AS: development of the research concept and design, conducting experiments, data analysis. BR: conducting laboratory studies, processing and interpretation of results, statistical analysis, manuscript writing. AS: conducting laboratory studies, analysis of the obtained data, manuscript editing. BR, AS: data processing consultation and verification. All authors have read and approved the final version of the article.

Information of funding

This research is funded by the Science Committee of the Ministry of Science and Higher Education of the Republic of Kazakhstan for 2024-2026 years (Grant No. AP23485181).

References

1 Astafyev, V., Ivanchenko, P., Kirkilevskiy, V. (2017). Effectiveness assessment of methods for moisture accumulation during winter precipitation in the arid steppe of Northern Kazakhstan. *Journal of Engineering and Applied Sciences*, 12(S4), 6821-6828. DOI: 10.36478/jeasci.2017.6821.6828.

2 Baktybekov, K. S., Aimbetov, A., Rakhimzhanov, B.K., Murat, A. (2020). Modeling of flood inundation for Zhabay River Basin in Central Kazakhstan Region. *Eurasian Physical Technical Journal*, 17(1), 157-162. DOI:10.31489/2020No1/157-162.

3 Beven, K. J., Kirkby, M. J. (1979). A physically based, variable contributing area model of basin hydrology. *Hydrological Sciences Journal,* 24(1), 43-69. DOI: 10.1080/02626667909491834.

4 Brooks, R. H., Corey, A. T. (1966). Properties of porous media affecting fluid flow. *Journal of the Irrigation and Drainage Division*, 92(2), 61-88. DOI: 10.1061/JRCEA4.0000425.

5 Dobrovol'ski, G. V., Balabko, P. N., Stasyuk, N. V., Bykova, E. P. (2011). Alluvial soils of river floodplains and deltas and their zonal differences. *Arid Ecosystems*, 1, 119-124. DOI: 10.1134/S207909611103005X.

6 Wang, J., Huang, H., Ariyasena, H. H. S., Zhao, J., Zhang, X., Gao, X., Zhao, X., Zhao, Y. (2025). A UAV-based method for root zone soil moisture modeling of different farmland scale with grain and economic crops. *Agricultural Water Management*, 321, 109932. DOI: 10.1016/j.agwat.2025.109932.

7 Food and Agriculture Organization of the United Nations. (n.d.). (2026). *Soil classification.* https://www.fao.org/soils-portal/data-hub/soil-classification/en/.

8 Gardner, W. R. (1958). Some steady-state solutions of the unsaturated moisture flow equation with application to evaporation from a water table. *Soil Science*, 85(4), 228-232. DOI: 10.1097/00010694-195804000-00006.

9 Gedroiz, K. K. (1931). Exchangeable cations of the soil and the plant: I. *Soil Science*, 32(1), 51-64. DOI: 10.1097/00010694-193107000-00005.

10 Mantoglou, A., Gelhar, L. W. (1987). Stochastic modeling of large-scale transient unsaturated flow systems. *Water Resources Research*, 23(1), 37-46. DOI: 10.1029/WR023i001p00037.

11 Hugenholtz, C. H., Whitehead, K., Brown, O. W., Barchyn, T. E., Moorman, B. J., LeClair, A., Riddell, KDA., Hamilton, T. K. (2013). Geomorphological mapping with a small unmanned aircraft system (sUAS): Feature detection and accuracy assessment of a photogrammetrically derived digital terrain model. *Geomorphology*, 194, 16-24. DOI: 10.1016/j.geomorph.2013.03.023.

12 Klute, A. (1952). A Numerical Method for Solving the Flow Equation for Water in Unsaturated Materials. *Soil Science*, 73(2), 105-116. DOI: 10.1097/00010694-195202000-00003.

13 Кулешова, А. (2021). Почвы Казахстана. WORLD OF NAN. https://world-nan.kz/blogs/v-kazakhstane-62-pashen-imeyut-nizkoe-soderzhanie-gumusa.

14 Муромцев, Н.А., Семенов, Н.А., Анисимов, К.Б. (2016). Особенности влагопотребления и влагообеспеченности растений различных экологических групп. *Бюллетень Почвенного института им. В.В. Докучаева*, 82, 71-87. DOI:10.19047/0136-1694-2016-82-71-87.

15 Oniga, V.E., Loghin, A.-M., Macovei, M., Lazar, A.-A., Boroianu, B., Sestras, P. (2024). Enhancing LiDAR-UAS derived digital terrain models with hierarchic robust and volume-based filtering approaches for precision topographic mapping. Remote Sensing, 16(1), 78. DOI: 10.3390/rs16010078.

16 Philip, J. R. (1957). The theory of infiltration: 1. The infiltration equation and its solution. *Soil Science,* 83(5), 345-357. DOI: 10.1097/00010694-195705000-00002.

17 Шеин, Е. В. (2016). Теоретические основы гидрологии почв в трудах А. А. Роде и современные подходы к описанию движения и равновесия. *Бюллетень Почвенного института имени В. В. Докучаева*, 83, 11-21. DOI: 10.19047/0136-1694-2016-83-11-21.

18 Terekhov, A., Muratova, N. (2002). Soils spring productive moisture reserve evaluation model for northern Kazakhstan on the basis of NOAA/AVHRR information. *Proceedings of SPIE*, 4542, 47-52. DOI: 10.1117/12.454202.

19 Stark, J. R., Fridley, J. D. (2022). Topographic drivers of soil moisture across a large sensor network in the USA. *Water Resources Research*, 59(7), e2022WR034315. DOI: 10.1029/2022WR034315.

20 Tauro, F., Porfiri, M., Grimaldi, S. (2016). Surface flow measurements from drones. *Journal of Hydrology*, 540, 240-245. DOI: 10.1016/j.jhydrol.2016.06.012.

21 Whelan, B. M., McBratney, A. B. (2012). Downscaling for site-specific mapping. *In Proceedings of the 5th Global Workshop on Digital Soil Mapping*, 353-356. DOI: 10.1201/b12728-69.

22 Zaslavsky, D., Sinai, G. (1981). Surface hydrology: I Explanation of phenomena. *Journal of the Hydraulics Division (ASCE)*, 107(1), 1-16. DOI: 10.1061/JYCEAJ.0005591.

23 Zhang, D., Zhao, Y., Qi, H., Shan, L., Chen, G., Ning, T. (2024). Effects of micro-topography and vegetation on soil moisture on fixed sand dunes in Tengger Desert, China. *Plants,* 13(11), 1571. DOI: 10.3390/plants13111571.

24 Жумагулов, И.И. (2021). Влияние атмосферных осадков на урожайность яровой пшеницы и ячменя в сухостепной зоне Северного Казахстана. *Исследования, результаты*, 3(91), 28-36. DOI: 10.37884/3-2021/04.

25 FAO SOILS PORTAL. *Soil classification*. https://www.fao.org/soils-portal/data-hub/soil-classification/en/

References

1 Astafyev, V., Ivanchenko, P., Kirkilevskiy, V. (2017). Effectiveness assessment of methods for moisture accumulation during winter precipitation in the arid steppe of Northern Kazakhstan. *Journal of Engineering and Applied Sciences*, 12(S4), 6821-6828. DOI: 10.36478/jeasci.2017.6821.6828.

2 Baktybekov, K.S., Aimbetov, A., Rakhimzhanov, B.K., Murat, A. (2020). Modeling of flood inundation for Zhabay River Basin in Central Kazakhstan Region. *Eurasian Physical Technical Journal,* 17(1), 157-162. DOI:10.31489/2020No1/157-162.

3 Beven, K.J., Kirkby, M.J. (1979). A physically based, variable contributing area model of basin hydrology. *Hydrological Sciences Journal*, 24(1), 43-69. DOI:10.1080/02626667909491834.

4 Brooks, R.H., Corey, A.T. (1966). Properties of porous media affecting fluid flow. Journal of the Irrigation and Drainage Division, 92(2), 61-88. DOI:10.1061/JRCEA4.0000425.

5 Dobrovol'ski, G.V., Balabko, P.N., Stasyuk, N.V., Bykova, E.P. (2011). Alluvial soils of river floodplains and deltas and their zonal differences. *Arid Ecosystems*, 1, 119-124. DOI: 10.1134/S207909611103005X.

6 Wang, J., Huang, H., Ariyasena, H.H.S., Zhao, J., Zhang, X., Gao, X., Zhao, X., Zhao, Y. (2025). A UAV-based method for root zone soil moisture modeling of different farmland scale with grain and economic crops. *Agricultural Water Management*, 321, 109932. DOI: 10.1016/j.agwat.2025.109932.

7 Food and Agriculture Organization of the United Nations. (n.d.). (2026). Soil classification. https://www.fao.org/soils-portal/data-hub/soil-classification/en/

8 Gardner, W.R. (1958). Some steady-state solutions of the unsaturated moisture flow equation with application to evaporation from a water table. *Soil Science*, 85(4), 228-232. DOI: 10.1097/00010694-195804000-00006.

9 Gedroiz, K.K. (1931). Exchangeable cations of the soil and the plant: I. *Soil Science*, 32(1), 51-64. DOI: 10.1097/00010694-193107000-00005.

10 Mantoglou, A., Gelhar, L.W. (1987). Stochastic modeling of large-scale transient unsaturated flow systems. *Water Resources Research*, 23(1), 37-46. DOI:10.1029/WR023i001p00037

11 Hugenholtz, C.H., Whitehead, K., Brown, O.W., Barchyn, T.E., Moorman, B.J., LeClair, A., Riddell, K.D.A., Hamilton, T.K. (2013). Geomorphological mapping with a small unmanned aircraft system (sUAS): Feature detection and accuracy assessment of a photogrammetrically derived digital terrain model. *Geomorphology*, 194, 16-24. DOI: 10.1016/j.geomorph.2013.03.023.

12 Klute, A. (1952). A Numerical Method for Solving the Flow Equation for Water in Unsaturated Materials. *Soil Science*, 73(2), 105-116. DOI: 10.1097/00010694-195202000-00003.

13 Kuleshova, A. (2021). Pochvy Kazahstana. WORLD OF NAN. https://world-nan.kz/blogs/v-kazakhstane-62-pashen-imeyut-nizkoe-soderzhanie-gumusa. [*in Russ*].

14 Muromcev, N.A., Semenov, N.A., Anisimov, K.B. (2016). Osobennosti vlagopotrebleniya i vlagoobespechennosti rastenii razlichnyh ekologicheskih grupp. *Byulleten' Pochvennogo instituta im. V.V. Dokuchaeva*, 82, 71-87. DOI:10.19047/0136-1694-2016-82-71-87. [*in Russ*].

15 Oniga, V.-E., Loghin, A.-M., Macovei, M., Lazar, A.-A., Boroianu, B., Sestras, P. (2024). Enhancing LiDAR-UAS derived digital terrain models with hierarchic robust and volume-based filtering approaches for precision topographic mapping. *Remote Sensing,* 16(1), 78. DOI:10.3390/rs16010078.

16 Philip, J.R. (1957). The theory of infiltration: 1. The infiltration equation and its solution. *Soil Science*, 83(5), 345-357. DOI:10.1097/00010694-195705000-00002.

17 Shein, E.V. (2016). Teoreticheskie osnovy gidrologii pochv v trudah A.A. Rode i sovremennye podhody k opisaniju dvizheniya i ravnovesiya. *Byulleten' Pochvennogo instituta imeni V.V. Dokuchaeva*, 83, 11-21. DOI:10.19047/0136-1694-2016-83-11-21. [*in Russ*].

18 Terekhov, A., Muratova, N. (2002). Soils spring productive moisture reserve evaluation model for northern Kazakhstan on the basis of NOAA/AVHRR information. *Proceedings of SPIE*, 4542, 47-52. DOI:10.1117/12.454202.

19 Stark, J.R., Fridley, J.D. (2022). Topographic drivers of soil moisture across a large sensor network in the USA. *Water Resources Research*, 59(7), e2022WR034315. DOI:10.1029/2022WR034315.

20 Tauro, F., Porfiri, M., Grimaldi, S. (2016). Surface flow measurements from drones. *Journal of Hydrology*, 540, 240-245. DOI: 10.1016/j.jhydrol.2016.06.012.

21 Whelan, B.M., McBratney, A.B. (2012). Downscaling for site-specific mapping. *In Proceedings of the 5th Global Workshop on Digital Soil Mapping*, 353-356. DOI:10.1201/b12728-69.

22 Zaslavsky, D., Sinai, G. (1981). Surface hydrology: I Explanation of phenomena. *Journal of the Hydraulics Division (ASCE)*, 107(1), 1-16. DOI:10.1061/JYCEAJ.0005591.

23 Zhang, D., Zhao, Y., Qi, H., Shan, L., Chen, G., Ning, T. (2024). Effects of micro-topography and vegetation on soil moisture on fixed sand dunes in Tengger Desert, China. *Plants*, 13(11), 1571. DOI:10.3390/plants13111571.

24 Zhumagulov, I.I. (2021). Vliyanie atmosfernyh osadkov na urozhajnost' yarovoi pshenicy i yachmenya v suhostepnoi zone Severnogo Kazahstana. I*ssledovaniya, rezul'taty*, 3(91), 28-36. DOI:10.37884/3-2021/04. [*in Russ*].

25 FAO SOILS PORTAL. *Soil classification*. https://www.fao.org/soils-portal/data-hub/soil-classification/en/

Солтүстік Қазақстандағы агроалқаптарда жер бедері өзгергіштігінің топырақ ылғалдылығына әсері

Рахимжанов Б., Сидорик А.

Түйін

Алғышарттар мен мақсат. Кеңестік кезеңдегі жер ресурстарын жоспарлау жүйесінің нәтижесінде Солтүстік Қазақстандағы ірі агроалқаптар тарихи тұрғыда жер бедерінің ерекшеліктеріне емес, әкімшілік шекараларға сүйеніп бөлінген, бұл жартылай қуаң жағдайларда топырақ ылғалдылығының кеңістіктік әркелкілігін күшейтуі мүмкін. Зерттеудің мақсаты − БПЛА арқылы алынған жер бедері деректері мен in-situ датчиктерінің телеметриясын пайдаланып, өкілдік қара топырақты (чернозем) алқапта микрожер бедерінің топырақ ылғалдылығының таралуына әсерін сандық тұрғыда бағалау.

Материалдар мен әдістер. Зерттеу Қазақстан, Қостанай облысындағы № 64 сынақ алқабында (440 га) жүргізілді. Жоғары айырымды сандық жер бедері модельдері (СЖБМ) БПЛА фотограмметриясы (Mavic 2 Pro; 2024 ж. тамыз) негізінде жасалып, биіктік градиенттерін сипаттауға қолданылды. Sentek Drill & Drop типті алты зонд (0-60 см, 10 см қадам) биіктік диапазоны бойынша орнатылып, 2025 ж. Мамыр-қыркүйек аралығында әр 30 мин сайын көлемдік су мөлшерін (VWC) тіркеді; датчик телеметриясы сапалық бақылаудан өтіп, айлық орташа мәндерге агрегатталды. Биіктіктің әсері әр ай және әр тереңдік қабаты бойынша Пирсон және Спирмен корреляциялары, сондай-ақ ең кіші квадраттар әдісіндегі сызықтық регрессия арқылы бағаланды (VWC = a + b•Биіктік).

Нәтижелер. Зондтар орналасқан нүктелердегі биіктік айырмасы шағын болғанына қарамастан (~3 м), айлық орташа ылғалдылық биіктікпен тұрақты түрде орташа байланыс көрсетті, әсіресе маусымның басында және терең қабаттарда. Пирсон бойынша статистикалық мәнді байланыстар ($p < 0,05$) мамыр айында 10-20 см ($r = -0,95$; $b = -3,03$% VWC/м; $R^2 = 0,90$), 20-30 см ($r = -0,91$; $b = -1,87$%/м; $R^2 = 0,83$) және 50-60 см ($r = -0,86$; $b = -2,08$%/м; $R^2 = 0,73$) қабаттарында байқалды. Маусымда мәнді әсер 40-50 см ($r = -0,86$; $b = -1,47$%/м; R2 = 0,74) және 50-60 см ($r = -0,93$; $b = -2,67$%/м; $R^2 = 0,86$) қабаттарында сақталды, ал шілдеде 50-60 см қабатында ($r = -0,85$; $b = -1,82$%/м; $R^2 = 0,72$) анықталды. Бұл төмен микротопографиялық позицияларда ылғалдың жүйелі түрде жоғары болатынын көрсетеді.

Қорытынды. БПЛА-дан алынған жер бедері метрикаларын тереңдік бойынша ажыратылған топырақ ылғалдылығы телеметриясымен біріктіру ірі далалық агроалқаптарда тамыр аймағындағы су қорының микротопографиялық бақылаушыларын анықтауға мүмкіндік береді. Анықталған «биіктік-ылғалдылық» градиенттері алқапішілік зонирлеуді, ылғал үнемдеу шараларын нысаналы жоспарлауды және Солтүстік Қазақстандағы қашықтан зондтау өнімдерін (топырақ ылғалдылығы) интерпретациялаудың тұрақтылығын арттыруды қолдайды.

Кілт сөздер: топырақ; ылғалдылық; жер бедері биіктігі бойынша сегментация; топырақ ылғалдылығы телеметриясы; агроалқаптарды БПЛА-мен сканерлеу; Солтүстік Қазақстан.

Влияние вариаций рельефа на влажность почвы на агрополях Северного Казахстана

Рахимжанов Б., Сидорик А.

Аннотация

Предпосылки и цель. В результате советской системы планирования землепользования крупные агрополя Северного Казахстана исторически формировались по административным границам, а не по особенностям рельефа, что в полузасушливых условиях может усиливать неоднородность почвенной влаги. Цель исследования − количественно оценить, как микрорельеф влияет на распределение влажности почвы в репрезентативном чернозёмном поле на основе БПЛА-производных данных рельефа и телеметрии in-situ датчиков влажности.

Материалы и методы. Исследование выполнено на тестовом поле № 64 (440 га), Костанайская область, Казахстан. Высокодетальные цифровые модели рельефа (ЦМР) получены по данным фотограмметрии БПЛА (Mavic 2 Pro; август 2024 г.) и использованы для описания градиентов

№ 1 (129)/2026 ISSN 3135-243X, 3135-2448

высоты. Шесть зондов Sentek Drill & Drop (0-60 см, шаг 10 см) были установлены в диапазоне высот и регистрировали объёмную влажность (VWC) с интервалом 30 мин в период май-сентябрь 2025 г.; телеметрические данные прошли контроль качества и были агрегированы до среднемесячных значений. Влияние высоты оценивали аналитически для каждого месяца и каждого горизонта по глубине с использованием корреляций Пирсона и Спирмена и линейной регрессии методом наименьших квадратов (VWC = a + b•Высота).

Результаты. Несмотря на небольшой диапазон высот (~3 м в точках установки зондов), среднемесячная влажность почвы демонстрировала устойчивые умеренные связи с высотой, особенно в начале сезона и в более глубоких горизонтах. Статистически значимые зависимости по Пирсону ($p < 0,05$) выявлены в мае на глубинах 10-20 см ($r = −0,95$; $b = −3,03\%$ VWC на 1 м; $R^2 = 0,90$), 20-30 см ($r = −0,91$; $b = −1,87\%$ на 1 м; $R^2 = 0,83$) и 50-60 см ($r = −0,86$; $b = −2,08\%$ на 1 м; $R^2 = 0,73$). В июне значимые эффекты сохранялись на 40-50 см ($r = −0,86$; $b = −1,47\%$ на 1 м; $R^2 = 0,74$) и 50-60 см ($r = −0,93$; $b = −2,67\%$ на 1 м; $R^2 = 0,86$), а в июле − на 50-60 см ($r = −0,85$; $b = −1,82\%$ на 1 м; $R^2 = 0,72$), что указывает на систематически более влажные условия в пониженных микротопографических позициях.

Заключение. Интеграция метрик рельефа, полученных по данным БПЛА, с послойной телеметрией влажности почвы позволяет выявлять значимые микротопографические факторы, определяющие водообеспеченность корнеобитаемого слоя в крупных степных агрополях. Выявленные градиенты «высота-влажность» могут быть использованы для внутриполевого зонирования, адресных влагосберегающих мероприятий и более корректной интерпретации спутниковых продуктов влажности почвы в Северном Казахстане.

Ключевые слова: почва; влажность; сегментация по высоте рельефа; телеметрия влажности почвы; БПЛА-съёмка агрополей; Северный Казахстан.

Appendixes (A-F) Sentek Soil Sensors telemetry

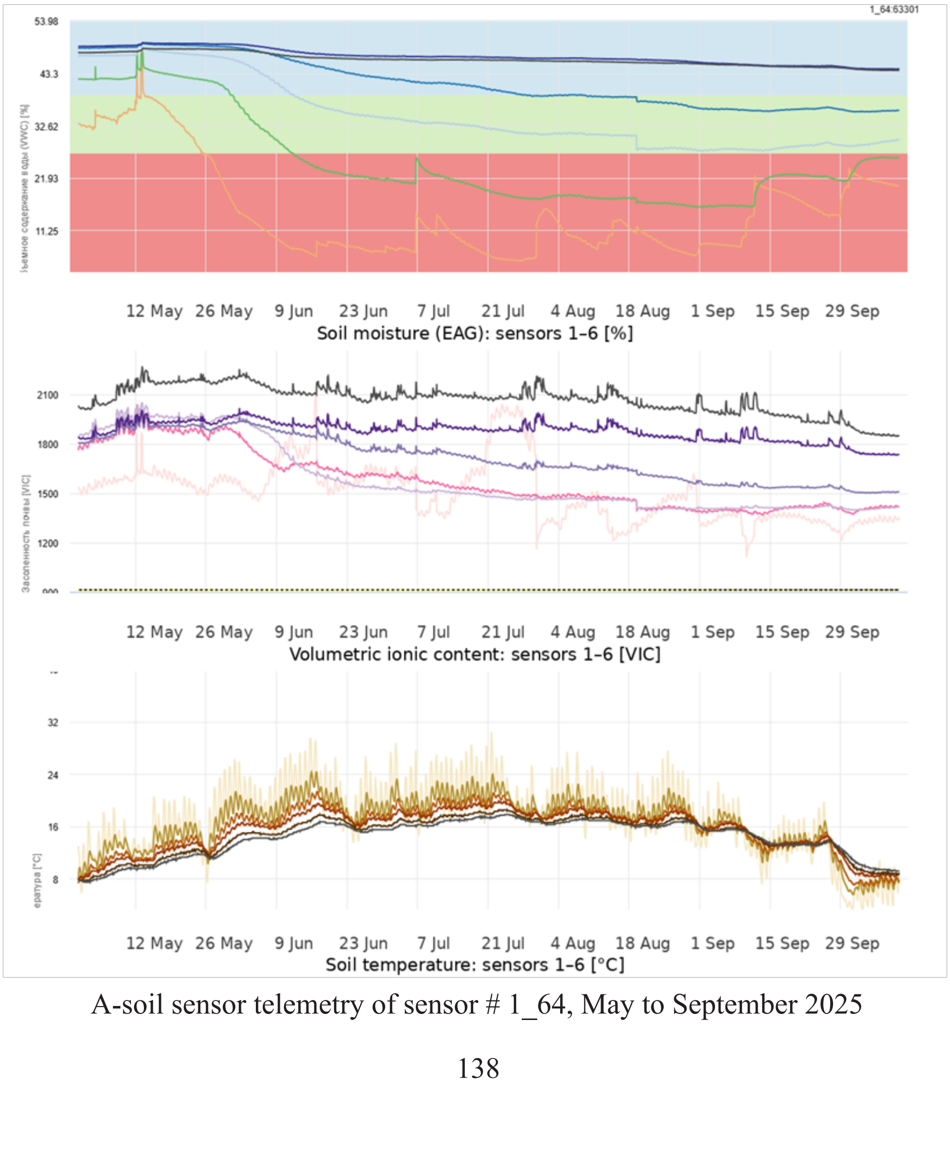

A-soil sensor telemetry of sensor # 1_64, May to September 2025

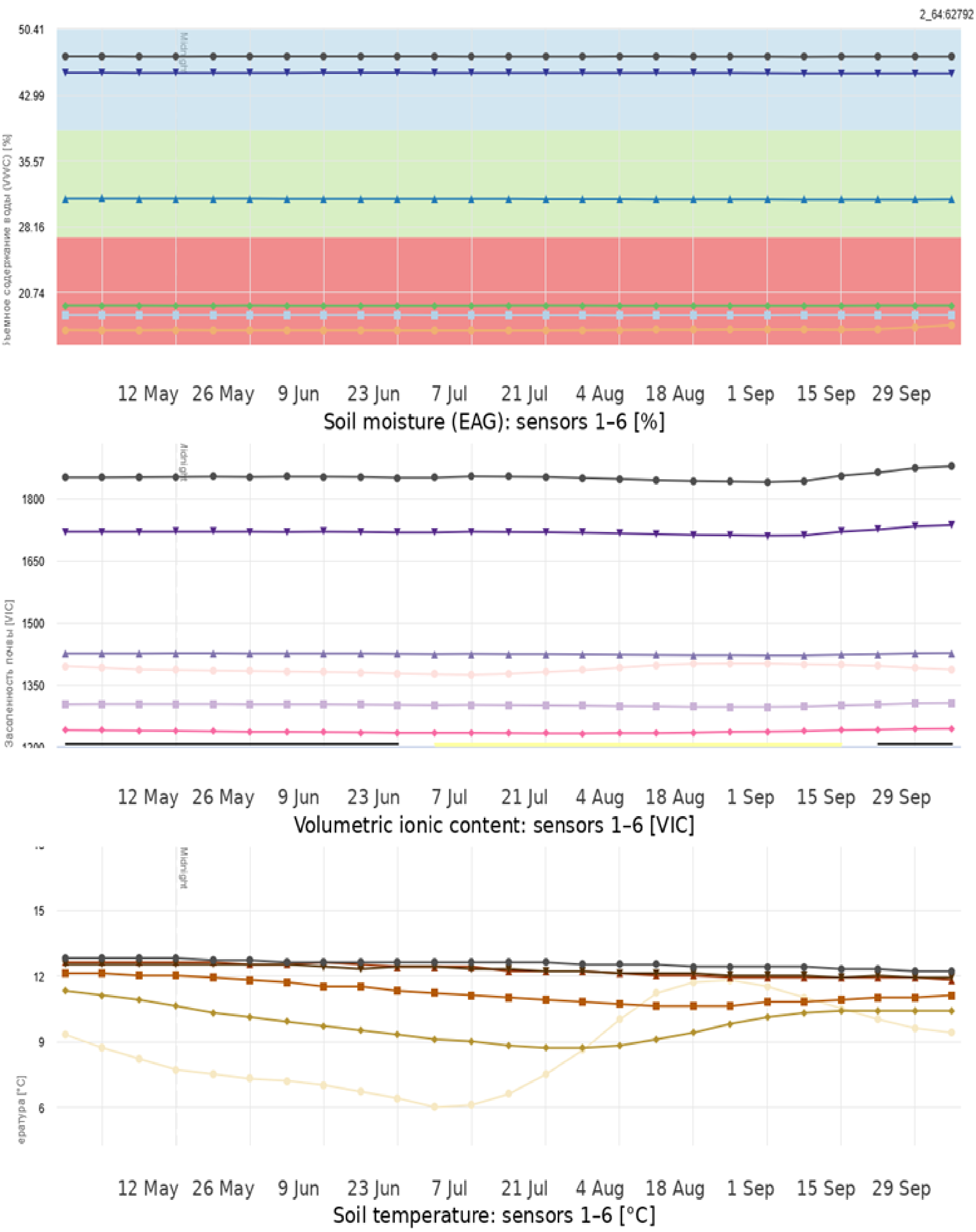

B-soil sensor telemetry of sensor # 2_64, May to September 2025

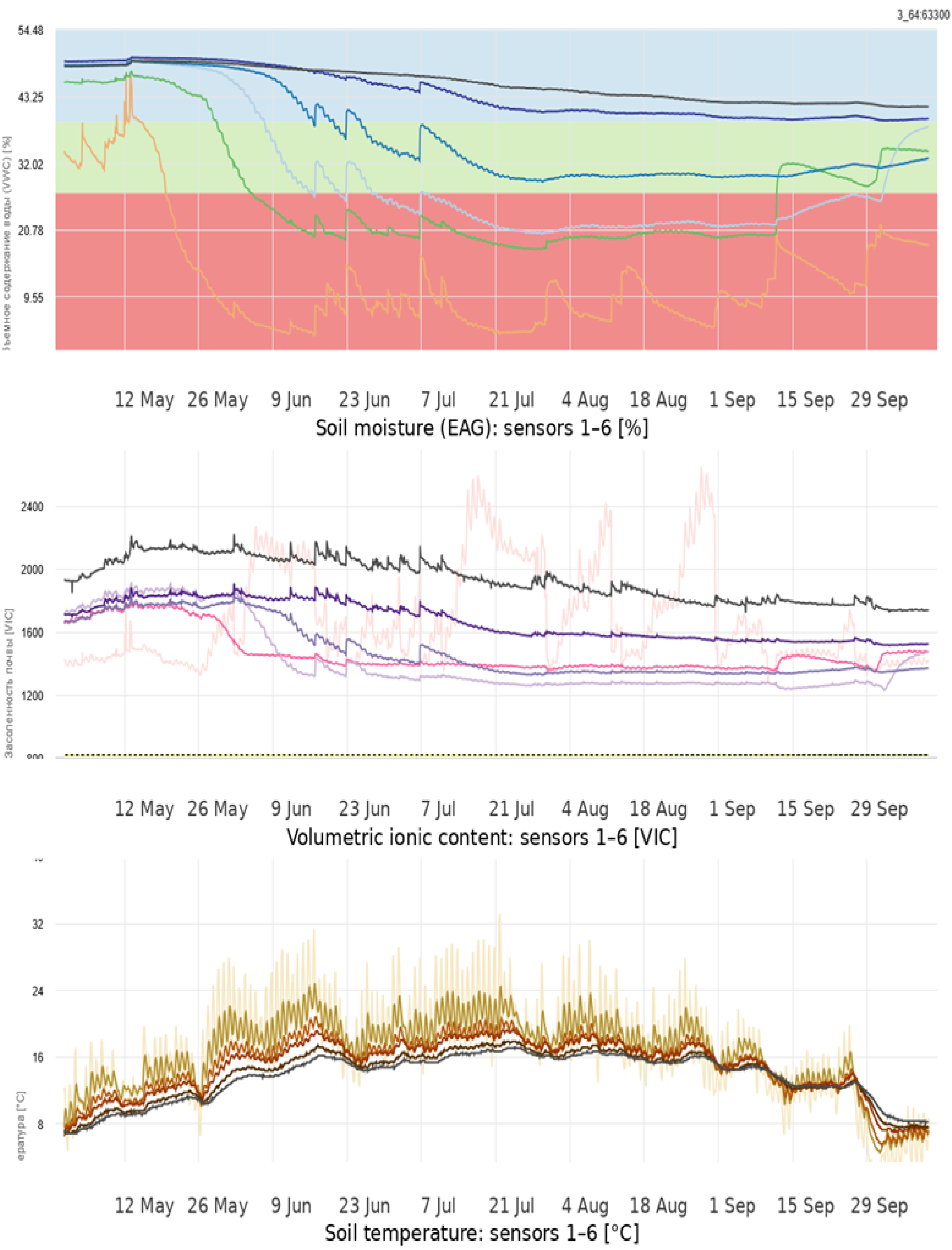

C-soil sensor telemetry of sensor # 3_64, May to September 2025

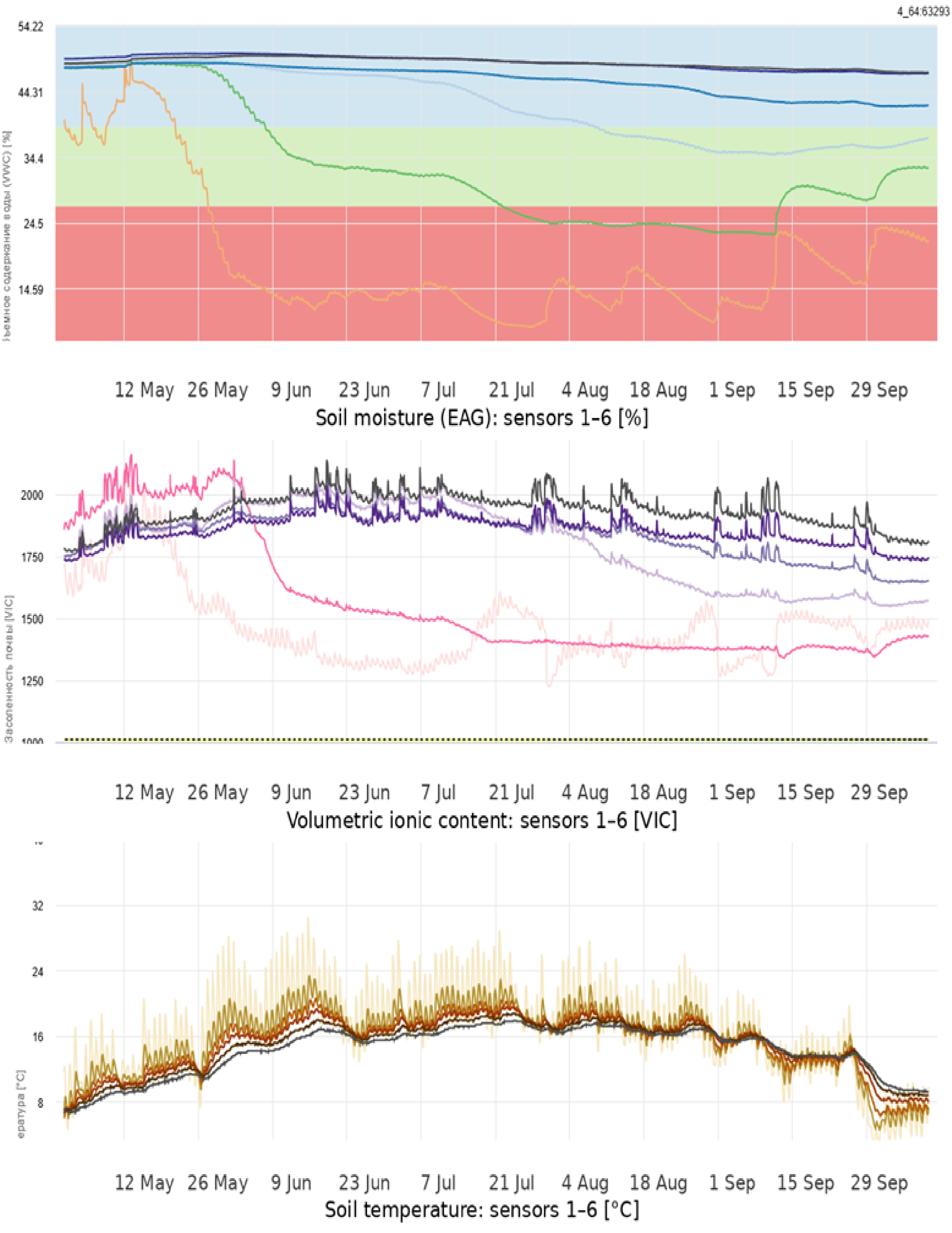

D-soil sensor telemetry of sensor # 4_64, May to September 2025

№ 1 (129)/2026 ISSN 3135-243X,3135-2448

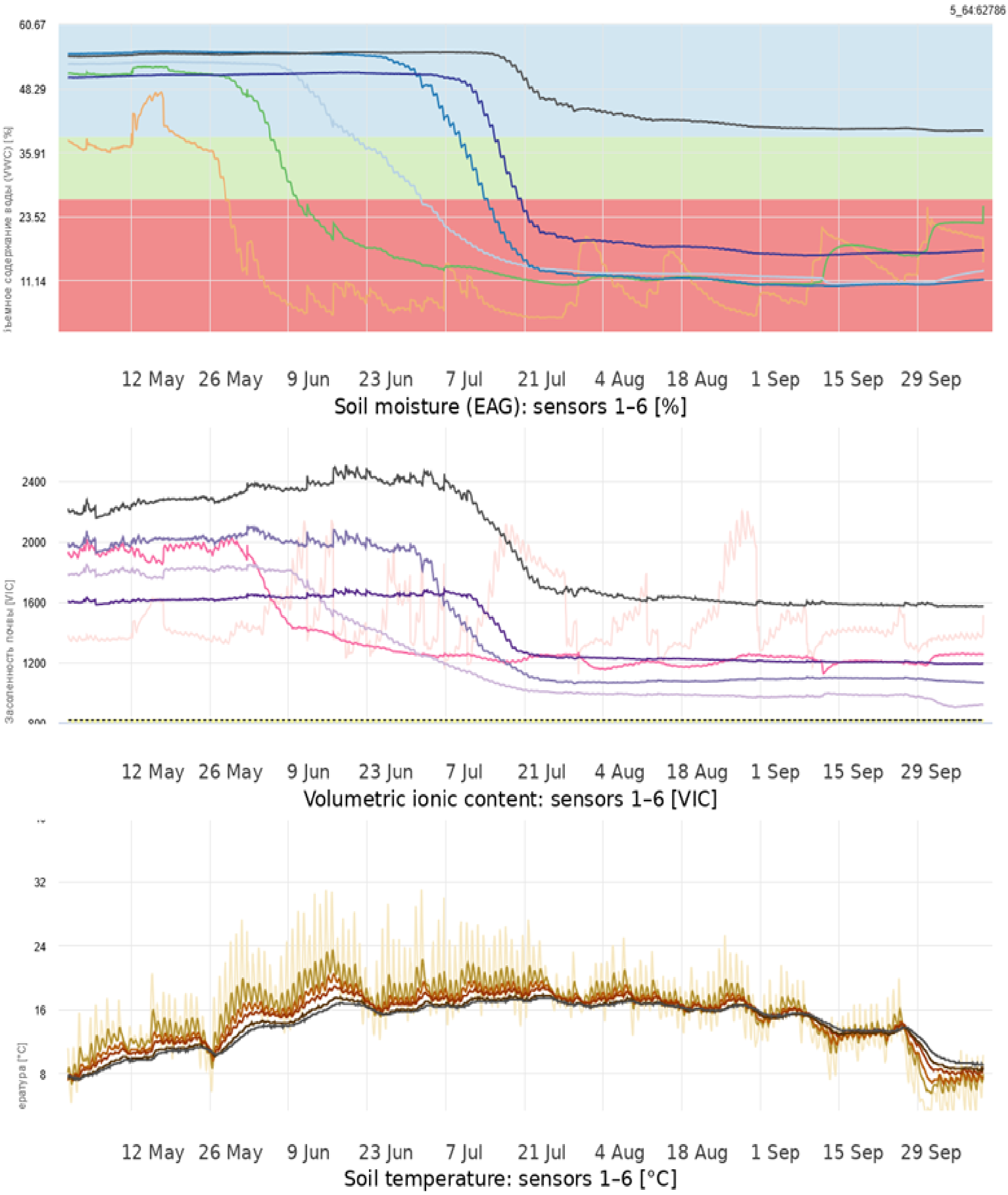

E-soil sensor telemetry of sensor # 5_64, May to September 2025

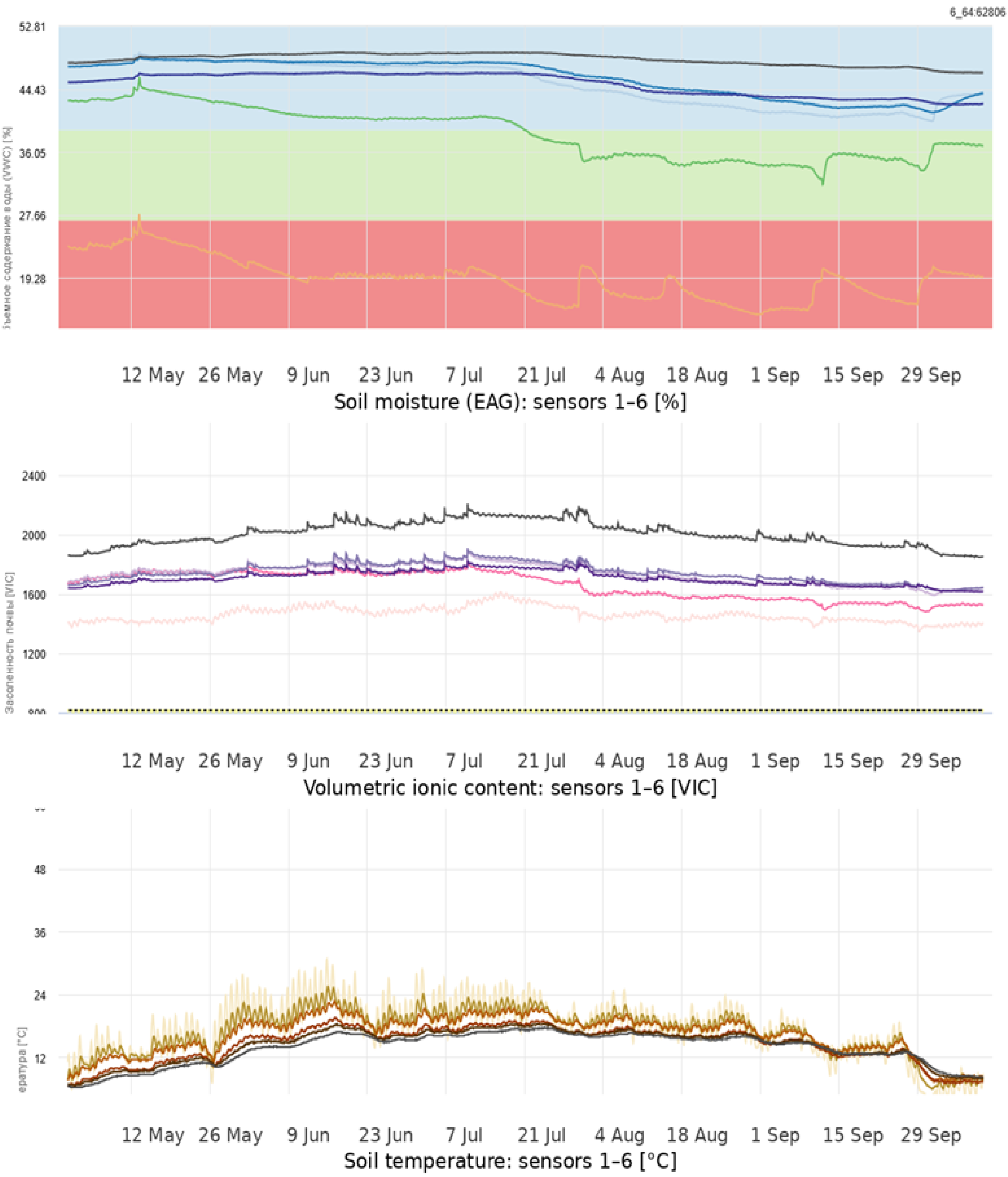

F-soil sensor telemetry of sensor # 6_64, May to September 2025